Korean J. Chem. Eng., 32(1), 88-96 (2015)
DOI: 10.1007/s11814-014-0168-2

pISSN: 0256-1115
eISSN: 1975-7220

Cadmium removal from aqueous solutions by pumice and nano-pumice

Sara Haddadi Khorzughy*,†, Teymur Eslamkish*, Faramarz Doulati Ardejani, and Mohammad Reza Heydartaemeh*****

*Department of Mining and Metallurgical Engineering, Amirkabir University of Technology, 424 Hafez Ave, Tehran, Iran
**School of Mining, College of Engineering, University of Tehran, Iran
***MSc of Mining Engineering, Shahrood University of Technology, Shahrood, Iran
(*Received 14 June 2013 • accepted 19 June 2014*)

Abstract−Use of low-cost minerals to eliminate mining and industrial pollutants is the main goal of this study. We investigated the ability of pumice and nano-pumice to remove cadmium from a synthetic aqueous solution. Batch experiments were performed to investigate adsorption characteristic; therefore, the effective factors influencing the adsorption process including solution pH, contact time and initial concentration have been considered. Equilibrium data were attempted by Langmuir and Freundlich isotherm models to realize the interaction between adsorbent and adsorbate. The results show that cadmium adsorption on Pumice follows the Langmuir isotherm model with a R^2 of 0.9996 and shows a homogeneous and mono-layer adsorption. Whereas, cadmium adsorption on nano-Pumice follows a Freundlich model (R^2=0.9939) and exhibits a multi-layer adsorption. The maximum mono-layer capacity (q_{max}) of cadmium for pumice and nano-pumice was calculated 26 and 200 mg/g, respectively. Two different kinetics models including pseudo first-order and pseudo second-order were studied to evaluate the rate and mechanism of cadmium adsorption by pumice and nano-pumice. The kinetics data indicate that a pseudo second-order model provides the best correlation of the experimental data.

Keywords: Adsorption, Pumice, Nano-pumice, Cadmium, Pollution, Aqueous Solutions

INTRODUCTION

Industries and mines are the most important producers of heavy metals and contamination sources in the environment. One of the widely used toxic metals, cadmium, belongs to the hazardous heavy metals group [1]. In nature, cadmium occurs in the form of cadmium sulfide (CdS), usually as a minor component in zinc, lead and copper ores [2]. During metal extraction and processing of zinc, lead and copper smelters, cadmium liberates and enters the environment as metal slag and dissolved form in wastewaters [2]. It is fairly mobile in soil but not biodegradable and is one of the hazardous pollutants for human life and biochemical cycles of organisms.

The consequences of the rapid growth of modern science and technology are environmental degradation and pollution problems. Therefore, the removal of heavy metals such as cadmium from contaminated water is essential to protect ecosystems and human health.

Although, various methods, including ion exchange, solvent extraction, reverse osmosis, precipitation and adsorption, have been applied to remove metal ions from aqueous solutions [3], most of these methods are not affordable due to high costs resulting in failure to remove low concentrations of metal ions and dispose of accumulated sludge after purification process. Among these methods, adsorption can be a suitable alternative approach to treat industrial waste water, especially if the used adsorbent is a low-cost material and it does not need pre-treatment. Adsorption is a physical-chemical process in which pollutants transfer from the aqueous phase to a solid phase. In recent decades, researchers have used many minerals as low-cost adsorbents with high adsorption efficiencies such as zeolite [4,5], Montmorillonite [6-8], kaolinite [8,9], diatomite [10-12] and perlite [13,14] to remove heavy metals and organics pollutions. Table 1 compares the adsorption capacities of various minerals including pumice and nano-pumice used in this study.

One of these low-cost minerals that can be used as adsorbent is pumice, which is abundant in many countries such as Iran (west and northwestern Iran). Pumice is a volcanic glass with high pores formed during explosive eruptions [15]. It typically has light color and silicic or felsic to intermediate composition. This volcanic rock has received significant interest because of its large surface area, high water adsorption capacity and surfaces with negative charge [16]. Literature review shows that few researches have been carried out to apply pumice as an adsorbent [1,16].

Panuccio et al. [1] performed batch experiments to evaluate the combined effects of ionic activity, pH, and contact time on the cadmium sorption in three different mineral adsorbents comprising vermiculite, zeolite, and Pumice. The results show that the equilibrium data followed both the Langmuir and Freundlich isotherm models. A pseudo second-order kinetics model fitted well to the experimental data for the adsorption process by three adsorbents. The results further indicate that the maximum adsorption capacity of pumice was lower than that of two other adsorbents. The adsorp-

†To whom correspondence should be addressed.
E-mail: Shaddadi@aut.ac.ir

Table 1. Comparison of the adsorption capacities of various minerals as adsorbents used for metal removal from aqueous solutions

Adsorbent	Metal ions	Maximum adsorption capacity (mg/g)	Source
Pumice	Cd^{2+}	26	Present study
Nano-Pumice	Cd^{2+}	200	Present study
Montmorillonite	Ni^{2+}	12.886	[6]
Montmorillonite	Cu^{2+}	7.616	[6]
Kaolinite	Cd^{2+}	9.9	[8]
Montmorillonite	Cd^{2+}	32.7	[8]
Bentonite	Cd^{2+}	9.3	[8]
Montmorillonite	Cd^{2+}	6.784	[7]
Montmorillonite	Pb^{2+}	32.89	[7]
Montmorillonite	Cu^{2+}	17.094	[7]
Montmorillonite	Zn^{2+}	22.727	[7]
Clinoptilolite	Cd^{2+}	0.082 (meq/g)	[4]
Scolecite	Cd^{2+}	0.0078 (meq/g)	[4]
Bigadic clinoptilolite	Cd^{2+}	0.0053 (meq/g)	[4]
Montmorillonite	Pb^{2+}	0.68	[9]
Montmorillonite	Cd^{2+}	0.72	[9]
Kaolinite	Pb^{2+}	0.12	[9]
Kaolinite	Cd^{2+}	0.32	[9]
Zeolite	Cu^{2+}	141.12	[5]
Zeolite	Co^{2+}	244.13	[5]
Zeolite	Cd^{2+}	118 (μmol/g)	[1]
Vermiculite	Cd^{2+}	143 (μmol/g)	[1]
Pumice	Cd^{2+}	47 (μmol/g)	[1]
Diatomite	Cd^{2+}	16.08	[12]
Diatomite	Pb^{2+}	24.94	[12]
Pumice	Ni^{2+}	1.187	[16]
Scoria	Ni^{2+}	0.98	[16]
Perlite	Pb^{2+}	8.906	[13]
Perlite	Cd^{2+}	0.64	[14]

tion capacity of three minerals depended upon pH and was independent of the initial cadmium concentration. However, the experiments were conducted without agitation. This most probably caused that the percentage of cadmium adsorption by pumice was obtained after six weeks. In their research, very slight amount of cadmium was adsorbed.

Alemayehu and Lennartz [16] investigated the removal of Ni (II) from water using volcanic rock grains including scoria and pumice. The experiments were conducted under batch conditions. The effect of pH, temperature, contact time, adsorbent/solution ratio, particle size and initial concentrations on the adsorption process was considered. The maximum adsorption capacities of 980 and 1,187 mg/kg were obtained for Ni(II) on scoria and pumice, respectively. The pseudo second-order equation well described the adsorption kinetics of Ni(II). In addition, the Langmuir and the Freundlich isotherm models well suited the equilibrium data. However, the surface characteristics of the adsorbents were not investigated.

There is therefore a need to investigate the adsorption efficiency of this widely available and low-cost material in detail. One of the greatest advantages of the present research over the previous studies applying pumice as adsorbent is that the effect of adsorbent particle size on adsorption process was considered. In this study, pumice was crushed into nano-size in order to efficiently use its surface feature for cadmium uptake from aqueous solution. The purpose of present work was to investigate the mechanism of Cd^{2+} adsorption onto pumice and nano-pumice. We evaluated the maximum adsorption capacities of Pumice and nano-Pumice and compared their application as a low-cost adsorbent with each other. In addition, the adsorption kinetics, isotherm and maximum adsorption capacity are discussed.

MATERIALS AND METHODS

1. Preparation of Adsorbent

1-1. Pumice Preparation

Pumice used in these experiments was taken from Malar Mining Company. To obtain homogeneous samples, raw pumice was crushed without washing process or initial preparation at two stages in mineral processing laboratory of Amirkabir University of Technology, Tehran, Iran. In the first stage, pumice samples were crushed by a mill jaw to reach particles with sizes less than 20 mm. Then, in the second stage, crushed samples were powdered by a Micronizer to reach 150 μm in size. The powdered pumice samples were finally used as adsorbent to adsorb cadmium ions from an aqueous solution.

1-2. Nano-pumice Preparation

To prepare nano-pumice, powdered pumice samples were ground by a planetary Ball mill (FRITSCH EQ-PC1-12) in Institute for Color Science and Technology, Tehran, Iran, to reach particles less than 100 nm in size and used as adsorbent in this research.

2. Characteristics of Adsorbent

2-1. X-ray Fluorescence Analysis

Chemical composition of pumice sample was determined by using X-ray fluorescence, XRF, (Philips X-Ray Diffractometer Xunique Π) in the Central Laboratory of Amirkabir University of Technology.

The results for this analysis are given in Table 2. As seen, the XRF

Table 2. Results of XRF analysis, density and color of pumice samples of Malar Mine

Compound	Percent %
SiO_2	58.08
Al_2O_3	16.32
Fe_2O_3	3.98
CaO	3.28
MgO	1.5
TiO_2	0.76
P_2O_5	0.52
Na_2O	3.91
K_2O	4.29
L.O.I	4.94
Density	0.5-0.7 g/cm^3
Color	Light gray-Dark gray

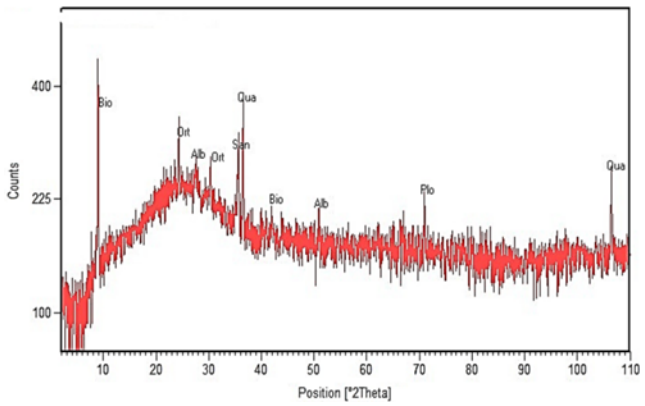

Fig. 1. XRD patterns of pumice samples used in this study.

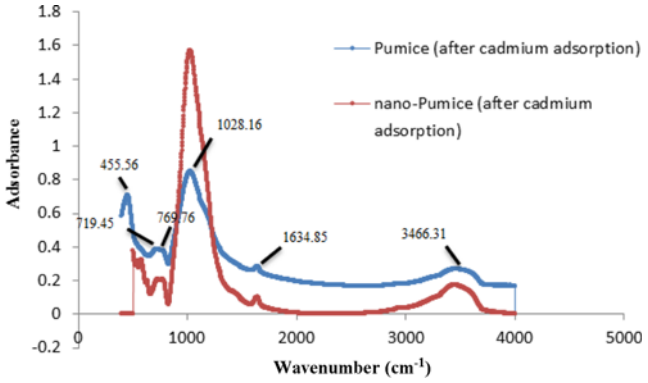

Fig. 3. FTIR spectra of Pumice and nano-Pumice after adsorption of Cd^{2+} ions.

experiment reveals that pumice is composed mainly of SiO_2 and Al_2O_3.

2-2. X-ray Diffraction

X-Ray diffraction (XRD) study using a Philips X-Ray Diffractometer Xunique 1140 was performed to indicate the minerals existing in pumice samples. Fig. 1 shows the XRD pattern. According to Fig. 1, minerals including Biotite (Bio), Orthoclase (Ort), Albite (Alb), Sanidine (San), quartz (Qua), Phlogopite (Plo) exist in the pumice sample. As this figure shows, Biotite, Quartz and Orthoclase are the main compounds of pumice. Diffraction peaks of Biotite occurred in the angles (2θ) range between 8.9430° and 41.9857° and peaks of orthoclase located in the range of 23.1019° and 30.6392°. In addition, major peaks of Albite, Quartz, Sanidine and Phlogopite are associated with the diffraction angles of 27.814°, 35.6016°, 36.5140° and 70.997°, respectively.

Results of XRF and XRD analyses suggest that unsaturated functional groups [$Si(OH)_x^{-n}$] and [$Al(OH)_y^{-m}$] can play an important role in adsorption of Cd^{2+} ions from aqueous solution by pumice and nano-pumice. It is because in surface hydroxyl groups the silicon atoms on the surface tend to maintain their tetrahedral coordination with oxygen. So, they have a tendency to adsorb metal ions with positive charges [14].

2-3. FTIR Analysis

The functional groups of natural pumice were confirmed using the Fourier transform infrared (FTIR) analysis ($5*10^{-5}<\lambda<4*10^{-4}$ nm, Perkin Elmer, USA). The capability for the adsorption of Cd^{2+} ions was studied to demonstrate its practicability as a cationic model compounds to investigate the adsorption behavior [17-19]. In this work, the FTIR analysis was in the range between 390 and 4,000 cm^{-1} to investigate the adsorbent properties. Fig. 2 shows the FTIR spectra of pumice and nano-pumice before adsorption process.

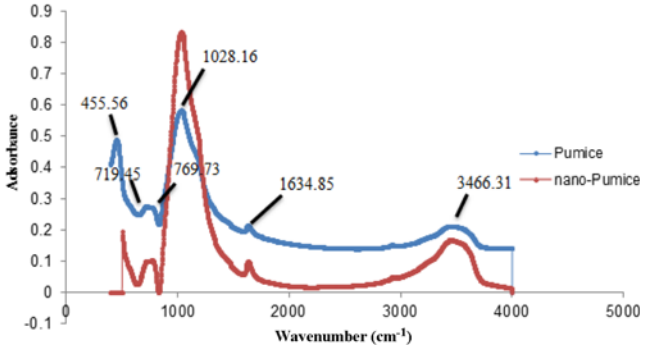

Fig. 2. FTIR spectra of Pumice and nano-Pumice before adsorption of Cd^{2+} ions.

The locations of peaks to exhibit adsorption bands were indicated at 455.56 cm^{-1} (stretch vibration of band Si-O-Al), 719.45 cm^{-1} (showing symmetric and bent of Quartz), 769.73 cm^{-1} (showing stretch vibration of band Si-O-H), 1,028.00 cm^{-1} (symmetric and stretch of band Si-O-Si), 1,634.85 cm^{-1} (stretch vibration of band H-O-H) and 3,466.31 cm^{-1} (broad and stretch of band O-H). Comparison of the FTIR spectra of pumice and nano-pumice indicates that all peaks of FTIR spectra of pumice show the same overview for nano-pumice. It means that the FTIR spectra of pumice and nano-pumice show the same trend before the adsorption process. However, the intensity of peaks for nano-pumice decreased rather than pumice. The cause of this phenomenon may be attributed to fewer nano-pumice particles.

The results of FTIR analysis of pumice and nano-pumice samples are compared in Fig. 3 for after the adsorption process. Comparing Figs. 2 and 3, one can say that the FTIR spectra of pumice and nano-Pumice show almost same trend before and after cadmium adsorption, but adsorption of cadmium increased the intensity of peaks.

2-4. Scanning Electron Microscopy

The morphology and other surface characteristics of pumice and nano-pumice were characterized by scanning electron microscopy (Philips SEM.XL30). Also, in this study, scanning electron microscopy images were used to measure the particle size of nano-pumice. The SEM results, given in Fig. 4, illustrate the difference of surface and texture morphology between pumice and nano-pumice. According to Fig. 4(a), pumice has a rough surface with amorphous structure, while Fig. 4(b) shows surface of sorbent with spherical and average particles size of 80 nm. It is obvious that nano-pumice has more numbers of pore space than pumice where Cd^{2+} ions can be trapped and adsorbed into these pores.

2-5. Atomic Force Microscopy

To investigate the surface characteristics of the adsorbent in more detail and to measure the particle size of nano-pumice, the atomic

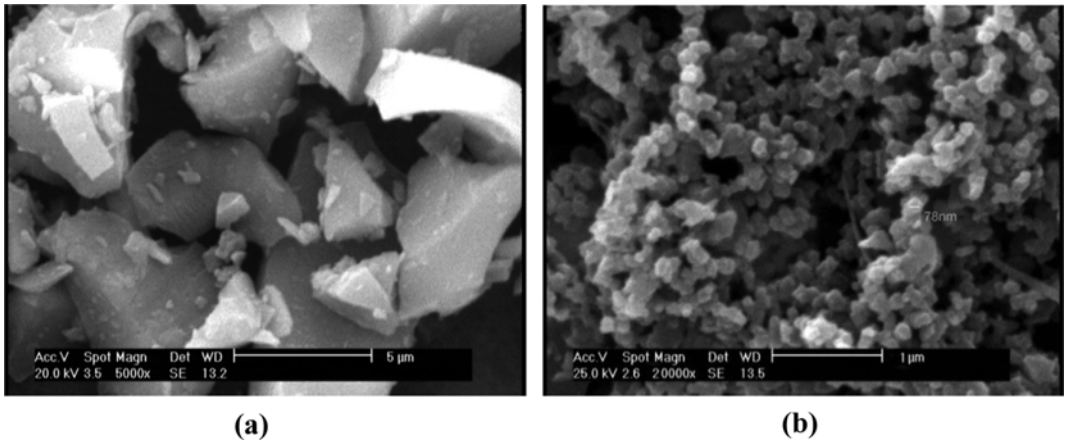

Fig. 4. Scanning electron microscopy of Pumice (a) and nano-Pumice (b).

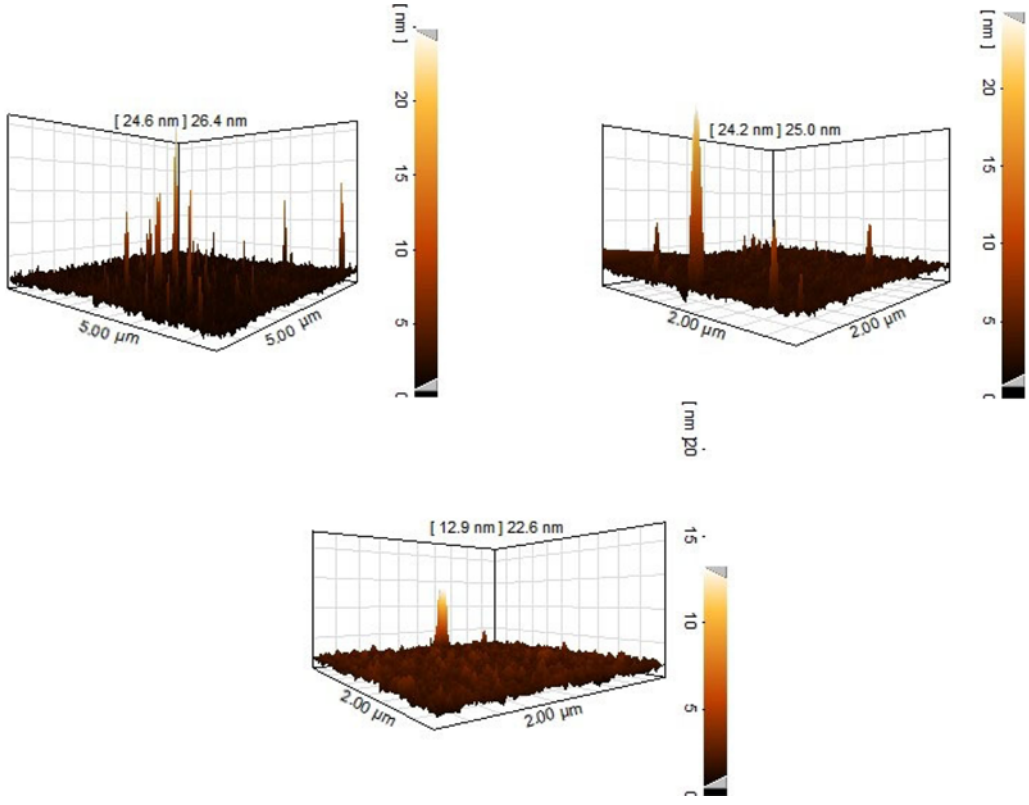

Fig. 5. Three dimensional AFM images from the surface of nano-Pumice.

force microscopy (AFM) observations were performed using DS-95-50E. AFM provides us microscopic information on the surface structure and plots the surface topography of the adsorbent [20]. Fig. 5 shows three-dimensional AFM images from the surface of nanoparticles.

According to Fig. 5, the average grain size of crushed samples varied between 22.6 and 26.4 nm. The color range shows the morphological changes of the surface, which indicate the adsorption sites on surface of nano-pumice and show the high capacity of nano-pumice in the adsorption process.

The results of SEM and AFM analyses indicated sizes less than 100 nm for particles of crushed pumice samples (nano-pumice).

3. Cadmium Solution

The main cadmium solution was prepared using $3CdSO_4 \cdot 8H_2O$. This was obtained from Merck Company of Germany. Cadmium solutions were measured by atomic absorption spectroscopy reference solutions for cadmium. Cadmium salt was dissolved in distilled water to make a 1,000 mg/*l* solution. Then, cadmium solutions were diluted using distilled water to prepare all the cadmium solutions used in these experiments. Cadmium concentrations of other solutions were measured by atomic adsorption spectroscopy (AAS) (Uni-Com9330).

4. Adsorption Procedure

Adsorption of Cd^{2+} from aqueous solution by pumice and nano-pumice was probed in batch experiments. Hence, effects of pH, contact time and initial concentration of metal solution were studied. The main solution was diluted to obtain the required concentrations (25, 50, 100, 200, 300 and 500 mg/*l*). In these experiments all containers were shaken at 500 rpm to homogenize and facilitate the reaction, and all these experiments were conducted at lab temperature (25±1 °C). Kinetic experiments were performed with constant pumice and nano-pumice dose, separately (0.1 g) at certain time intervals (10, 20, 30, 45, 60, 90, 120 and 180 min) and pH=6.

The adsorption isotherm experiments were conducted by mixing 0.1 gr of pumice and nano-pumice separately in a jar containing 50 ml of Cd^{2+} solutions with varying concentrations (50, 100, 200, 300, 400 and 500 mg/*l*) at pH=6 for 120 min to attain equilibrium condition. Initial kinetic experiments indicate that adsorption time of 120 min was sufficient to reach equilibrium. Therefore, 120 min of mixing was selected for all batch isotherm experiments.

After the experiments, the solids were separated from solutions by filtering and then residual cadmium concentration was analyzed by AAS. Following this, amount of adsorbed per unit mass of adsorbent, q_e (mg/g), was calculated using Eq. (1) [21]:

$$q = \frac{C_0 - C_e}{M} \times V \tag{1}$$

where, q, C_0, C_e, V and M are the amount of adsorbed per unit mass of adsorbent (mg/g), initial metal concentration (mg/*l*), equilibrium concentration of metal (mg/*l*), used volume of solution (L) and dosage of adsorbent (mg), respectively.

4-1. Adsorption Kinetics

The kinetic parameters are essential to predict the rate of adsorbate uptake on adsorbent from aqueous solution in order to design and model an appropriate treatment system based on adsorption process [14,22-26]. In this study, to examine the rate of the adsorption process, the kinetic of the adsorption data was analyzed using two different kinetic models: the pseudo-first order and pseudo-second order models, which can be expressed in their linearized forms as Eqs. (2) and (3), respectively [27]:

$$\ln(q_e - q_t) = \ln q_e - K_1 t \tag{2}$$

$$\frac{t}{q_t} = \frac{1}{K_2 q_e^2} + \frac{1}{q_e} t \tag{3}$$

where, q_t (mg/g) is the adsorption uptake at time t (min): q_e (mg/g) denotes the adsorption capacity at adsorption equilibrium; and K_1 (min^{-1}) and K_2 ($g \cdot mg^{-1} \cdot min^{-1}$) are the kinetic rate constants for the pseudo-first order and pseudo-second order models, respectively.

4-2. Equilibrium Experiments

The most common method of presenting adsorption equilibrium data is the adsorption isotherm, which describes the equilibrium sorption of a material on adsorbent surface at constant temperature. It expresses the concentration adsorbate in the solid phase q as a function of adsorbate concentration in liquid phase C [28]. The two widely used Langmuir and Freundlich isotherm equations were applied to fit the equilibrium data to predict the equilibrium parameters of adsorption system.

The Langmuir isotherm is applied to describe a single-solute system. This model suggests that adsorption occurs at homogeneous sites by monolayer sorption with no significant interaction between adsorbed ions [29]. The linear form of the Langmuir equation is expressed as follows [29,30]:

$$\frac{C_e}{q_e} = \frac{1}{q_m b} + \frac{1}{q_m} C_e \tag{4}$$

where, C_e is the equilibrium concentration of adsorbate (mg/*l*), q_e denotes the equilibrium amount of metal ions adsorbed per unit mass of adsorbent (mg/g), q_m and b represent the maximum adsorption capacity (mg/g) and the Langmuir isotherm constant (*l*/mg), respectively. A linear plot of C_e/q_e against C_e, gives a straight line with a slope of $1/q_m$ and an intercept of $1/q_m b$ [29,30].

The Freundlich model was also applied to investigate the adsorption isotherm of cadmium ions on pumice and nano-pumice. The Freundlich equation is used for heterogeneous systems and considers multilayer adsorption [29,30]. The Freundlich model is expressed as follows [30]:

$$q_e = K_f C_e^{1/n} \tag{5}$$

The linear form of this model is [29]:

$$\log q_e = \log K_f + \frac{1}{n} \log C_e \tag{6}$$

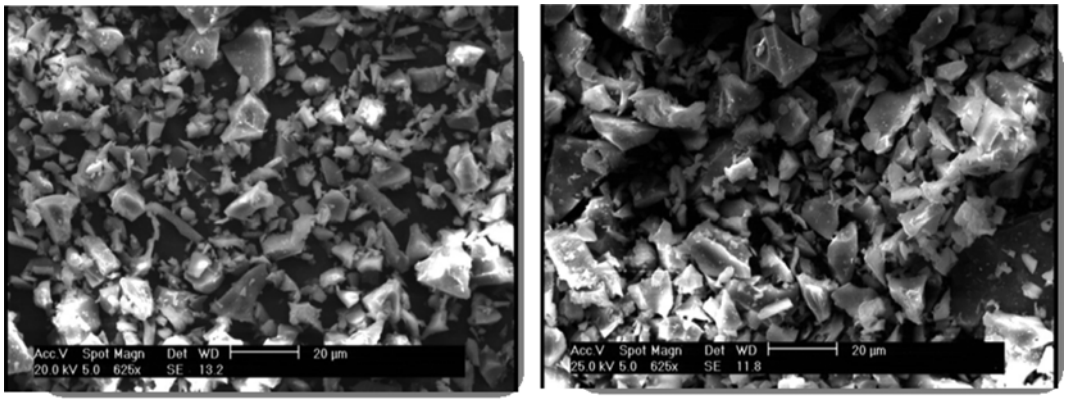

(a) (b)

Fig. 6. SEM images of Pumice surface before (a) and after (b) cadmium adsorption.

where q_e is the number of metal ions adsorbed per unit mass of adsorbent (mg/g), C_e denotes equilibrium concentration of metal ions (mg/*l*), K_f and n represent Freundlich constants related to the adsorption capacity and adsorption intensity, respectively.

Freundlich parameters K_f and n can be calculated from the intercept and slope of a linear plot with $\log q_e$ versus $\log C_e$ [29].

RESULTS AND DISCUSSION

1. Interpretation of SEM Images

Scanning electron micrographs of pumice before and after adsorption of cadmium are shown in Fig. 6(a), (b). From Fig. 6(a), that Pumice had a porous surface with irregularly shaped particles. As is seen in Fig. 6(b), the surface of pumice slightly changed after cadmium adsorption, and the porous surfaces were fewer than those of the prior to the adsorption process. The reason is that the cadmium ions were adsorbed on the external surfaces of pumice.

The SEM images of nano-pumice surface before and after cadmium adsorption are shown in Fig. 7(a), (b). According to Fig. 6(a) and Fig. 7(a), nano-pumice has significant numbers of pore spaces in comparison with the pumice surface, wherein the cadmium ions can be trapped. This characteristic makes nano-pumice a sufficient adsorbent. As evident from Fig. 7(b), the surface structure of nano-pumice clearly changed after cadmium adsorption, and porous surfaces were almost totally occupied with the cadmium ions. In other words, the adsorption made a uniform surface with a non-porous structure for nano-pumice. This phenomenon can be attributed to the sticking of nanoparticles of pumice by cadmium ions, because the nanoparticles of pumice and cadmium ions have negative and positive charges, respectively.

2. Effect of pH

The pH of solution is one of the most important factors in the adsorption process, especially adsorption capacity [28]. To investigate the effect of pH, 0.1 g of adsorbent (pumice and nano-pumice separately) was added to 50 ml of cadmium solution with concentration of 100 mg/*l*, at lab temperature and agitating speed of 500 rpm with various initial pH values of 2, 3, 4.5, 6, 7, 8.5 and 10 for pumice and 2, 3, 5, 7 and 9 for nano-pumice for 120 min.

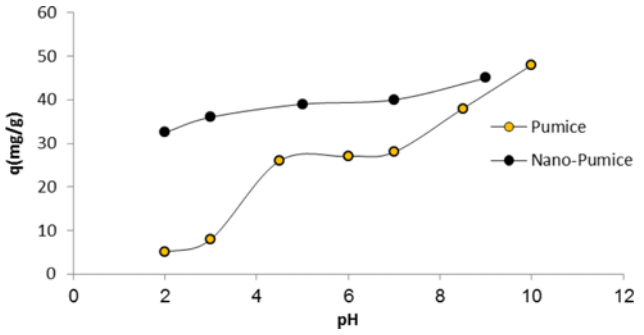

Fig. 8. Effect of pH on cadmium adsorption ob Pumice and nano-Pumice. Condition: amount of adsorben: 0.1 g, initial cadmium concentration: 100 mg/*l*, T=25±1 °C and agitating speed=500 rpm.

The relationship between pH values and the amount of Cd^{2+} adsorbed on pumice and nano-pumice is presented in Fig. 8. At any pH, Cd^{2+} adsorbed on nano-pumice shows higher adsorption capacity than that on pumice, which shows the high capacity of nano-pumice for the removal of cadmium ions from aqueous solutions.

According to this figure, cadmium adsorption increased from 5 to 48 mg/g for pumice while for nano-pumice, Cd^{2+} adsorption increased from 32.5 to 45 mg/g as pH increased. For both adsorbents, the amount of Cd^{2+} adsorbed increased slightly above pH=7. This phenomenon can be explained by precipitation of Cd^{2+} as insoluble $Cd(OH)_2$ precipitate. Therefore, pH values beyond 7 were not studied for other experiments to avoid the formation of Cd^{2+} precipitates as the hydroxides.

As mentioned before (Table 2), the oxides of Fe, Al, Si, Ca and Mg are present in varying amounts in pumice. The hydroxylated surface of these oxides develops a charge on the adsorbent surface in aqueous solution [16]. Hence, the variation of adsorbed Cd^{2+} at various pHs can be explained by the oxides present in adsorbents [14,16]. Little Cd^{2+} uptake at low pH values shows that functional oxide groups (Al_2O_3, Fe_2O_3, SiO_2) of the adsorbent are protonated. Furthermore, additional protons compete with Cd^{2+} ions for the same binding site [14,16]. However, in an alkaline medium, a neg-

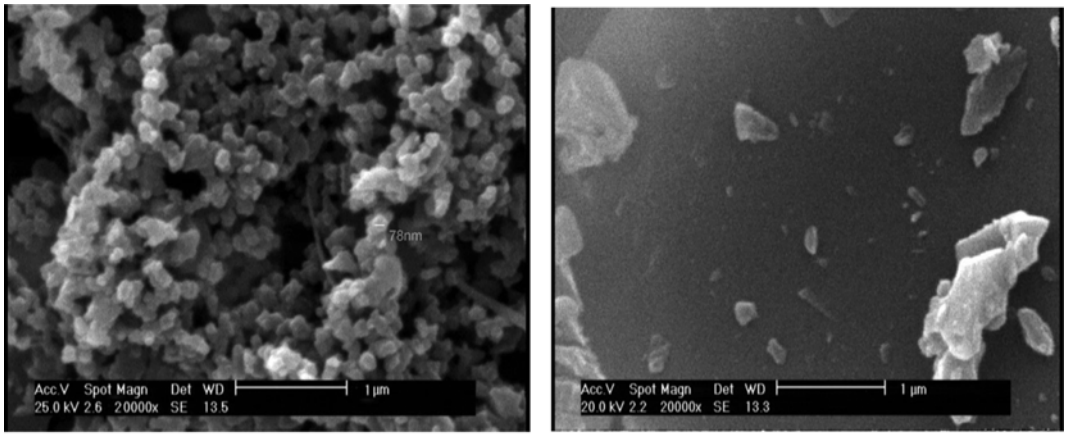

Fig. 7. SEM images of nano-Pumice surface before (a) and after (b) cadmium adsorption.

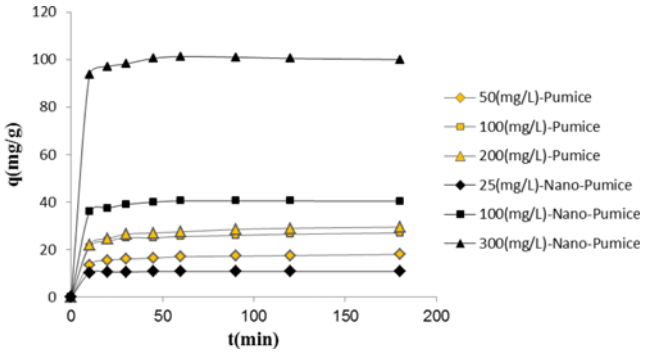

Fig. 9. Amount of cadmium adsorption onto Pumice and nano-Pumice at three diffrent concentrations as function of contact time. Conditions: amount of adsorbent: 0.1 g, T=25± 1 °C, pH=6 and agitating speed=500 rpm.

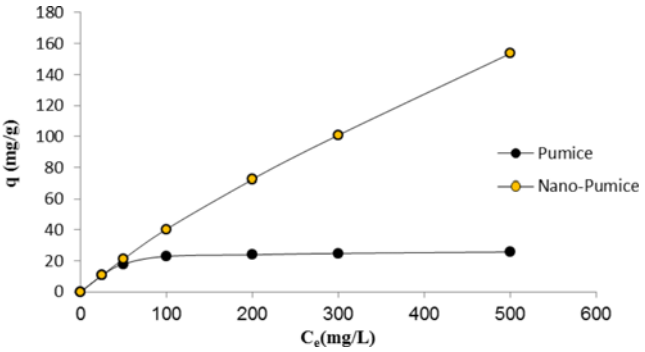

Fig. 10. Amount of cadmium adsorption onto Pumice and nano-Pumice for diffrent concentrations. Conditions: amount of adsorbent: 0.1 g, T=25±1 °C, pH=6 and agitating speed= 500 rpm.

ative charge develops on adsorbents surface, so the amount of adsorption increases significantly until the cadmium precipitates at pHs above 7 [14].

However, as Fig. 8 shows, for both adsorbents, the best adsorption took place at pH=6, which is close to the natural pH of pumice. So, this pH was selected for the subsequent experiments.

3. Kinetics Results

3-1. Effect of Contact Time on Cadmium Adsorption

The adsorption of cadmium onto pumice and nano-pumice at three different initial concentrations as a function of contact time is shown in Fig. 9. This figure indicates that the amount of cadmium adsorption by pumice and nano-pumice increases with time to attain equilibrium condition after 60 and 10 min, respectively, and it remains constant thereafter. It is also illustrated that with an increase in the initial cadmium concentration from 50 to 200 mg/*l* and 25 to 300 mg/*l*, the amount of cadmium adsorption, increases from 18 to 29.5 and 10.85 to 101.25 by pumice and nano-pumice, respectively.

The rapid rate of Cd^{2+} adsorption at the early minutes of adsorption process is the main point in this figure. In other words, more than 75% and 92% of cadmium adsorption by pumice and nano-pumice occurred at 10 min, respectively, which may be attributed to the availability of a large number of vacant adsorption sites on the adsorbent surfaces [29,30]. However, the remaining vacant surface sites are occupied with time due to repulsive forces between the adsorbate ions on the solid surface and in the bulk phase [29,30].

3-2. Adsorption Kinetics Results

The kinetics parameters of the pseudo-first and pseudo-second order models at different initial concentration of cadmium are given in Table 3 in which the correlation coefficient values for pseudo-second order model were found higher than 0.99 for cadmium adsorption by pumice and nano-pumice. In addition, as can be seen in this table, the theoretical q_e values are similar to the experimental q_{exp} values. Thus, the adsorption of Cd^{2+} on pumice and nano-pumice can be well described by the pseudo-second order kinetic model.

The K_2 values calculated from the pseudo-second order kinetic model for cadmium adsorption by pumice and nano-pumice decreased with an increase in cadmium concentration. It means that the rate of adsorption of Cd^{2+} onto pumice and nano-pumice decreases by increasing Cd concentration.

As further illustrated in this table, the K_2 values for cadmium concentration by nano-pumice were higher than those of pumice, which suggests that nano-pumice adsorbed cadmium ions faster than did pumice.

4. Equilibrium Results

4-1. Effect of Initial Concentration

The effect of initial concentration on adsorption of cadmium by pumice and nano-pumice is shown in Fig. 10. As cadmium concentration increased from 25 to 500 mg/*l*, the amount of cadmium adsorption by pumice increased and reached equilibrium amount (25.75 mg/g) for a concentration of 100 mg/*l*, while the cadmium uptake by nano-pumice increased from 10.8 to 153.6 mg/g.

However, the amount of cadmium adsorption increased with increasing the initial concentration of cadmium, but the efficiency of adsorption decreased (Fig. 11). The high amount of cadmium

Table 3. Kinetics parameters for cadmium adsorption by Pumice and nano-Pumice

Type of adsorbent	Initial concentration (mg/L)	q_{exp} (mg/g)	Pseudo first-order			Pseudo second-order		
			q_{e1} (mg/g)	K_1 (1/min)	$(r_1)^2$	q_{e2} (mg/g)	K_2 (g·mg^{-1}·min^{-1})	$(r_2)^2$
Pumice	50	18	2.9	0.012	0.6736	18.32	0.0125	0.9997
	100	27	7.9	0.014	0.6842	27.4	0.0098	0.9998
	200	29.5	10	0.02	0.7634	30.12	0.0071	0.9998
Nano-Pumice	25	10.85	2.32	0.007	0.2651	10.87	0.2	0.9999
	100	41.55	6.2	0.014	0.4768	40.52	0.012	0.9999
	300	101.25	9	0.014	0.3316	101.1	0.032	0.9999

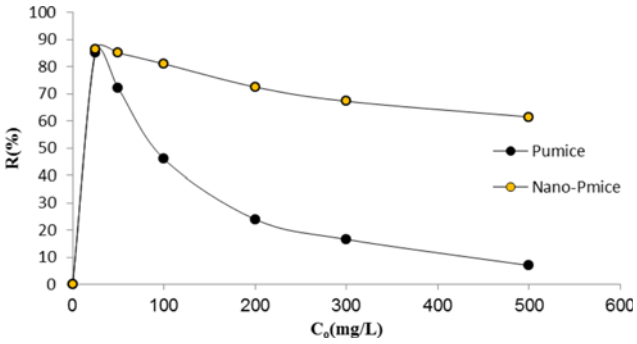

Fig. 11. Precentage of cadmium adsorption onto Pumice and nano-Pumice for diffrent concentrations. Conditions: amount of adsorbent: 0.1 g, T=25±1 °C, pH=6 and agitating speed= 500 rpm.

Table 4. Parameters of Longmuir and Freundlich for adsorption of cadmium by Pumice and nano-Pumice

Type of adsorbent	Langmuir			Freundlich		
	q_m (mg/g)	b (*l*/g)	R^2	n	K_f (*l*/mg)	R^2
Pumice	25.97	0.13	0.9996	5.82	9.975	0.8616
Nano-Pumice	200	0.0134	0.9435	1.56	5.505	0.9939

adsorption percentage by nano-pumice at 500 mg/*l* indicates the higher capacity of nano-pumice than pumice for adsorption of elevated concentration of cadmium.

4-2. Isotherm Results

To interpret the equilibrium data, experimental data were fitted to Langmuir and Freundlich isotherm models. The parameters of the Langmuir and Freundlich isotherms for Cd^{2+} adsorption on pumice and nano-pumice are given in Table 4.

As this table shows, the highest value of R^2 for Langmuir isotherm (0.9996) describes that the Cd^{2+} adsorption on Pumice was best represented by this model. According to this model, the maximum adsorption capacity, q_m, and the Langmuir constant, b, for adsorption process were calculated as 25.97 and 0.13, respectively. The highest R^2 value of Freundlich model (0.9939) shows that the adsorption of Cd^{2+} on nano-Pumice is described by this model. The values of n, which represent the favorability of the adsorption, were more than one, indicating that the adsorption of Cd^{2+} on nano-pumice was favorable.

Based on the Langmuir model, the value of maximum adsorption capacity for Cd^{2+} adsorption by nano-pumice was 200 mg/g, which shows the potential performance of nano-pumice for the removal of Cd^{2+} ions from aqueous solutions.

According to the results of isotherm studies, cadmium adsorption on pumice shows a homogeneous and monolayer adsorption, whereas cadmium adsorption on nano-pumice follows the Freundlich model and exhibits multi-layer adsorption.

CONCLUSION

As low-cost adsorbents, the pumice and nano-pumice were applied to remove cadmium ions from an aqueous solution. To use pumice surface feature more efficiently, the pumice samples were crushed at nano size and characterized by SEM and AFM analyses. The results of these analyses indicated sizes less than 100 nm for particles of crushed pumice samples. Adsorption experiments were carried out as a function of contact time, solution pH and initial metal ion concentration. The results show that cadmium adsorption by pumice and nano-pumice was pH dependent, and the optimum pH was 6. The results further show that the amount of cadmium adsorption increases with pH increasing until the cadmium ions precipitated as $Cd(OH)_2$ (at pHs above 7). In other words, the removal of cadmium ions in low pHs (acidic conditions) is less than that of in high pHs (basic media), which this fact can be explained on the basis of aqua complex formation of the oxides present on adsorbents surface. The kinetic studies for both adsorbents show that the adsorption process was well explained by pseudo second-order kinetic model. The isotherm studies reveal that the Langmuir model was the best-fitted model for the adsorption of cadmium by pumice (R^2= 0.9996). The maximum adsorption capacity of cadmium was 25.97 mg/g. Furthermore, the cadmium adsorption on nano-pumice followed the Freundlich model (R^2=0.9939). The results of isotherm studies indicate that by producing nano-particles from pumice and increasing the surface area of the adsorbent, the adsorption capacity increased from 25.97 to 200 mg/g. Accordingly, the nano-pumice was shown to be an efficient adsorbent and could be employed as a low-price adsorbent to eliminate metal ions from aqueous solutions.

REFERENCES

1. M. R. Panuccio, A. Sorgona, M. Rizzo and G. Cacco, *J. Environ. Manage.*, **90**(1), 364 (2009).
2. V. C. Srivastava, I. D. Mall and I. M. Mishra, *Chem. Eng. J.*, **117**(1), 79 (2006).
3. V. K. Gupta, C. K. jain, A. Imran, M. Sharma and V. K. Saini, *Water Res.*, **37**(16), 4038 (2003).
4. S. Wang and Y. Peng, *Chem. Eng. J.*, **156**(1), 11 (2010).
5. E. Erdem, N. Karapinar and R. Donat, *J. Colloid Interface Sci.*, **280**(2), 309 (2004).
6. C. O. Ijagbemi, M.-H. Baek and D. S. Kim, *J. Hazard. Mater.*, **166**(1), 538 (2009).
7. A. Sdiri, T. Higashi, T. Hatta, F. Jamoussi and N. Tase, *Chem. Eng. J.*, **172**(1), 37 (2011).
8. K. G. Bhattacharyya and S. S. Gupta, *Adv. Colloid Interface Sci.*, **140**(2), 114 (2008).
9. S. Babel and T. A. Kurniawan, *J. Hazard. Mater.*, **97**(1-3), 219 (2003).
10. K. Badii, F. Doulati Ardejani, M. Aziz Saberi, N. Yousefi Limaee and S. Z. Shafaei, Indian *J. Chem. Technol.*, **17**(1), 7 (2010).
11. B. Bahramian, F. Doulati Ardajani, V. Mirkhani and Kh. Badii, *Appl. Catal. A: Gen.*, **345**(1), 97 (2008).
12. M. A. M. Khraisheh, Y. S. Al-degs and W. A. M. Mcminn, *Chem. Eng. J.*, **99**(2), 177 (2004).
13. M. Irani, M. Amjadi and M. A. Mousavian, *Chem. Eng. J.*, **178**, 317 (2011).
14. T. Mathialagan and T. Viraraghavan, *J. Hazard. Mater.*, **94**(3), 291

(2002).
15. M. Kitis, S. S. Kaplan, E. Karakaya, N. O. Yigit and G. Civelekoglu, *Chemosphere*, **66**, 130 (2007).
16. E. Alemayehu and B. Lennartz, *Appl. Geochem.*, **25**(10), 1596 (2010).
17. Y. F. Lin, H. W. Chen, P. s. Chien, Ch. s. Chiou and Ch. Lio, *J. Hazard. Mater.*, **185**(2-3), 1124 (2011).
18. S. H. Huang and D. H. Chen, *J. Hazard. Mater.*, **163**(1), 174 (2009).
19. G. J. Churchman, W. P. Gates, B. K. G. Theng and G. Yuan, *Handbook of Clay Science*, **1**, 1 (2006).
20. T. Al-R. Khalid, K. A. Nada and J. Sh. Zainb, *Int. J. Electrochem. Sci.*, **8**, 5594 (2013).
21. D. Doulia, Ch. Leodopoulos, K. Gimouhopoulos and F. Rigas, *J. Colloid Interface Sci.*, **340**(2), 131 (2009).
22. C. K. Jain, *Hydrological Sci. J.*, **46**(3), 419 (2001).
23. J. Pedro Silva, S. Sousan, J. Rodrigues, H. Antuunes, J. Porter, I. Goncalves and S. Ferreira-Dias, *Sep. Purif. Technol.*, **40**(3), 309 (2004).
24. Z. r. Liu and S. q. Zhou, *Process Saf. Environ. Prot.*, **88**(1), 62 (2010).
25. H. Zaghouane-Boudiaf and M. Boutahala, *Int. J. Miner. Process.*, **100**(3-4), 72 (2011).
26. N. Tekin and Y. Ates, *Int. J. Miner. Process.*, **112-113**, 49 (2012).
27. M. G. Mostafa, Y.-H. Chen, J.-Sh. Jean, Ch.-Ch. Lio and Y.-Ch. Lee, *J. Hazard. Mater.*, **187**(1-3), 89 (2011).
28. F. Doulati Ardejani, Kh. Badii, N. Yousefi Limaee, S. Z. Shafaei and A. R. Mirhabibi, *J. Hazard. Mater.*, **151**(2-3), 730 (2008).
29. B. Al-Rashdi, Ch. Tizaoui and N. Hilal, *Chem. Eng. J.*, **183**, 294 (2012).
30. I. Y. Rushdi, El-E. Bassam and Ala'a H. Al-Muhtaseb, *Chem. Eng. J.*, **171**(3), 1143 (2011).